Abnormal lipoproteins in the ANIT-treated rat: a transient and reversible animal model of intrahepatic cholestasis

Jeffrey W. Chisholm and Peter J. Dolphin[1]

Lipoprotein Research Group, Department of Biochemistry, Dalhousie University, Halifax, Nova Scotia B3H 4H7, Canada

Abstract The α-naphthylisothiocyanate (ANIT)-treated rat was evaluated as a model for lipoprotein metabolism in cholestatic liver disease. Alterations in lipoprotein composition over a period of 120 h after ANIT treatment (100 mg/kg) were studied. Eighteen hours after treatment, plasma bilirubin and bile acid levels began to rise, together with significant increases in free cholesterol, C-18/16, C-18/18, and C-18/20 phospholipid molecular species. By 48 h, plasma lipid levels were maximal, free cholesterol was 935%, cholesteryl ester 294%, phospholipid 611%, and triacylglycerols 176% of controls, and the cholesteryl ester to free cholesterol ratio began to recover with a modest shift from cholesteryl esters containing C-20 fatty acids to those containing C-18 fatty acids. Lecithin:cholesterol acyltransferase activity was near normal, lipoprotein lipase activity was increased, and hepatic triacylglycerol lipase activity was decreased. Density gradient ultracentrifugation of rat plasma demonstrated a marked shift in lipoprotein density towards the low density lipoprotein range, with the increased lipid being associated with apolipoproteins A-I and E. The presence of large 300–400 Å particles and the high surface to core lipid ratio in this density range was consistent with the presence of lipoprotein-X-like vesicles. Apolipoprotein B-48 accumulation was observed in the high density fractions (d_{15} > 1.063 g/ml) suggesting that these rats have impaired lipoprotein remnant removal. All of these increased levels returned to near normal by 120 h. This study demonstrates that ANIT-treatment induces a transient, fully reversible, non-surgical intrahepatic cholestasis that results in many of the plasma lipoprotein abnormalities associated with human hepatic cholestasis and the bile duct-ligated rat.—**Chisholm, J. W., and P. J. Dolphin.** Abnormal lipoproteins in the ANIT-treated rat: a transient and reversible animal model of intrahepatic cholestasis. *J. Lipid Res.* 1996. **37:** 1086–1098.

Supplementary key words α-naphthylisothiocyanate (ANIT) • Lp-X • intrahepatic cholestasis • rats • density gradient ultracentrifugation • electrophoresis

Abnormalities in lipoprotein structure have been widely reported as primary or secondary manifestations of pathological and genetic diseases. Understanding the metabolic processes responsible for the synthesis and catabolism of these abnormal particles is often difficult using in vitro simulations alone, and in many cases in vivo study may be required for full elucidation of their metabolism. In this paper, we report our initial characterization of the α-naphthylisothiocyanate (ANIT)-treated rat as a novel animal model for the study of lipoprotein abnormalities in cholestasis.

A single dose of ANIT when given by gavage to rats, mice, and guinea pigs (1) produces a transient intrahepatic cholestasis (2, 3), necrosis of the bile duct endothelium, and areas of focal injury to the hepatocytes in periportal areas of the liver (4–6). The pharmacological action of ANIT remains unclear, but appears to be related to effects of the drug directly upon the hepatocytes and not bile canalicular cells (3). Microsomal mixed function and cytochrome P450 oxidase activities have been shown to be decreased (7, 8) together with their drug-metabolizing activities (7–9). Kosser et al. (6) have suggested that the onset of ANIT-induced cholestasis is biphasic. Initially, changes in hepatocanicular function and increased tight junction permeability are observed and these are followed by bile duct obstruction and hepatocellular dysfunction. The second phase appears to begin with near complete cessation of bile flow between 16 and 24 h (2, 6) which is followed by increased levels of bile components within the plasma compartment. Maximal plasma concentrations of bile acids (2, 6) are observed by 24 h (2, 7, 8), while conjugated bilirubin (10, 11) and liver enzymes are maximally elevated by 48 h (7, 8). These abnormal plasma levels return to near normal by 96 h (7). Krell, Hoke, and Pfaff (12)

Abbreviations: ANIT, α-naphthylisothiocyanate; LPL, lipoprotein lipase; HTGL, hepatic triacylglycerol lipase; LCAT, lecithin:cholesterol acyltransferase; TC, total cholesterol; CE, cholesteryl ester; FC, free cholesterol; PL, phospholipid; TAG, triacylglycerol; HDL, high density lipoprotein; LDL, low density lipoprotein; VLDL, very low density lipoprotein; Lp-X, lipoprotein X.

[1]To whom correspondence should be addressed.

have suggested that increased leakage in tight cell junctions around the bile ductules may be involved in the reflux of bile constituents into the plasma compartment.

Changes in plasma lipoproteins resulting from ANIT-induced cholestasis have not been extensively studied. Katterman and Wolfrum (13) have shown that ANIT treatment results in increased plasma free cholesterol and a decreased CE/FC ratio in the presence of increased LCAT activity. In the liver, both free and esterified cholesterol were elevated, but in contrast to plasma the CE/FC ratio was increased. This suggests that ANIT-induced intrahepatic cholestasis, like extrahepatic cholestasis in the rat, occurs under conditions were liver cholesterogenesis is up-regulated (14, 15). More recently, Mitamura (16), was able to demonstrate that ANIT-induced cholestasis resulted in large elevations of plasma phospholipid and free cholesterol, smaller increases in cholesteryl ester, little change in triacylglycerols, and the presence of phospholipid-rich HDL.

We have extended these initial studies of the altered plasma lipoproteins found in ANIT-induced cholestatic rats. Our goals were first, to investigate the ANIT-treated rat as a non-surgical model of human intrahepatic cholestasis; second, to define the alterations in lipid mass, density distribution, abnormal particles, and lipolytic enzyme activities in the plasma compartment of the ANIT-treated rat and compare them with those observed in the well-characterized bile duct-ligated rat (17, 18); and finally, to compare the alterations in lipoproteins with those occurring in various forms of human liver disease, LCAT deficiency, and Intralipid infusion, with the objective of evaluating the ANIT-treated rat as a suitable model for subsequent studies on the metabolism of abnormal lipoproteins.

MATERIALS AND METHODS

Animals

Female Sprague-Dawley rats (225–275 g) were used for all experiments. Rats were pair fed regular rat chow, given water ad libitum and housed under 12-h light/dark conditions. All rats were fasted for 12 h prior to treatment. Rats were lightly anesthetized by interperitoneal administration of Ketamine/Xylazine (3%/0.37% w/v) at a dosage of 0.8–1.0 ml/kg and given 100 mg/kg ANIT (Sigma, St. Louis, MO) in a 25 mg/ml corn oil (Mazola) bolus by gavage. Control rats received a similar amount of corn oil by weight. At the indicated experimental time points, fasted rats were deeply anesthetized by an interperitoneal injection of Ketamine/Xylazine 2.0–2.5 ml/kg and blood was collected from the descending aorta into tubes containing EDTA to a final concentration of 1 mg/ml. For postheparin plasma collection, blood was collected from fasted anesthetized rats 8 min after an interjugular injection of 100 U/kg sterile heparin (Sigma, St. Louis, MO) saline solution (150 U/ml, pH 7.4). Plasma was isolated by centrifugation at 3000 *g* for 30 min at 4°C. A preservative cocktail containing thimerosal (Sigma, St. Louis, MO), aprotinin (Sigma, St. Louis, MO), Na_2EDTA, and sodium azide was added to yield respective final concentrations of 0.005%, 0.001%, 0.01%, and 0.02%. PMSF (phenylmethylsulfonyl fluoride) (Sigma, St. Louis, MO), 0.035%, was also added to samples not being used for lipolytic enzyme determinations.

Enzymatic and lipid analysis

Aspartate aminotransferase (Boehringer Mannheim), alanine aminotransferase (Boehringer Mannheim), alkaline phosphatase (Boehringer Mannheim), bilirubin (Boehringer Mannheim), and bile acids (Sigma, St. Louis, MO) were measured manually using commercial kits as indicated. Total cholesterol, free cholesterol, triacylglycerols, and phospholipids were measured either directly by enzyme kits (Boehringer Mannheim) or by gas chromatographic total lipid profiling (19). When enzyme kits were used, cholesteryl ester mass was calculated from total cholesterol and free cholesterol by mole subtraction using an average rat cholesteryl ester molecular weight of 645 g/mol. All plasma samples were measured by gas chromatographic total lipid profiling, as an unidentified component of plasma from ANIT-treated rats completely inhibited the choline oxidase method of phospholipid determination used in the enzymatic kit. The enzymatic inhibition was not present

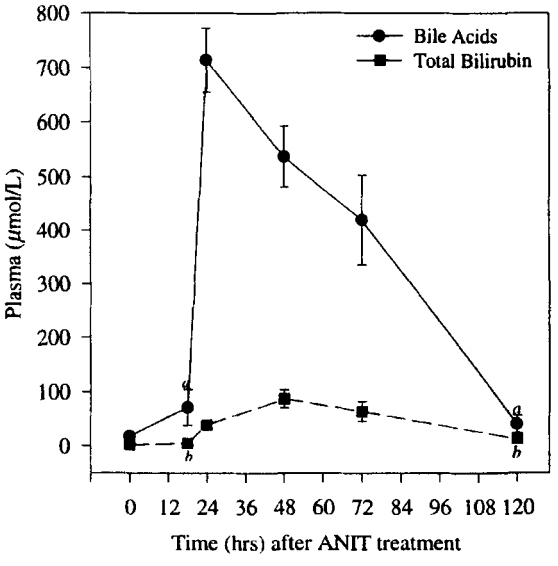

Fig. 1. Plasma total bile acids and bilirubin with respect to time after ANIT administration (100 mg/kg). Points shown are for fasted rats and are the mean ± SEM (n = 6). [a]Bile acids and [b]bilirubin measurements were not significant ($P < 0.05$) versus controls (0 h).

TABLE 1. Plasma markers of liver damage

	0 h	18 h	24 h	48 h	72 h	120 h
Alkaline phosphatase (I.U. @ 37°C)	53 ± 0[a]	-	-	214 ± 19[b]	-	-
Aspartate aminotransferase (I.U. @ 37°C)	103 ± 7	160 ± 39[c]	396 ± 37[c]	2513 ± 345d	1069 ± 120[d]	117 ± 10
Alanine aminotransferase (I.U. @ 37°C)	43 ± 6	65 ± 10[c]	210 ± 19[c]	1916 ± 312[d]	1130 ± 197[d]	76 ± 9

Values are given as mean ± SEM (n = 6 except where noted).
[a]n = 2.
[b]n = 10.
[c]n = 5.
[d]Significant ($P < 0.05$) versus controls (0 h).

in the lipoprotein positive fractions of plasma from treated rats after ultracentrifugation, suggesting that the unknown inhibitor was associated with the lipoprotein free (d > 1.21 g/ml) plasma components.

LCAT activity assays

LCAT activity was determined using the exogenous synthetic proteoliposome substrate method of Chen and Albers (20) as described by Jauhiainen and Dolphin (21).

Triacylglycerol lipase activity assays

Plasma triacylglycerol lipase activities were measured essentially by the method of Jackson and MacLean (22). The assay was performed on the day of plasma collection and all samples were determined in triplicate. To ensure that endogenous apolipoprotein C-II was not limiting in samples, pooled rat plasma was heat-inactivated at 62°C for 10 min to denature lipases (23) and a 20% assay volume was added to control and total lipase sample tubes as a source of apolipoprotein C-II. Hepatic triacylglycerol lipase was measured in the presence of 1 M NaCl to inhibit lipoprotein lipase. Lipoprotein lipase activity was calculated as the difference between total lipase and hepatic triacylglycerol lipase activities.

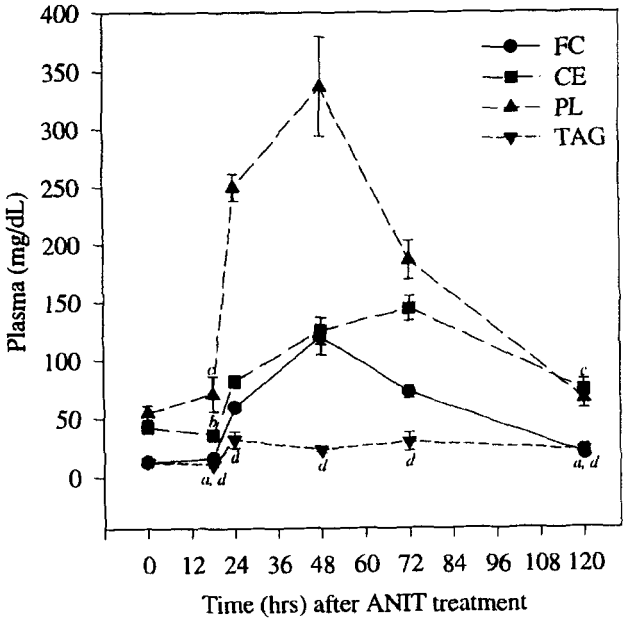

Fig. 2. Plasma lipids with respect to time after ANIT administration (100 mg/kg). Points shown are for fasted rats and are the mean ± SEM (n = 6). [a]Free cholesterol (FC), [b]cholesteryl ester (CE), [c]phospholipid (PL), and [d]triacylglycerol (TAG) measurements were not significant ($P < 0.05$) versus controls (0 h).

Immunoassay of plasma apolipoproteins

Rat plasma samples were assayed for apolipoproteins B, E, and A-I by electroimmunoassay as previously described by Krul and Dolphin (24).

Density gradient ultracentrifugation

Rat plasma samples to be analyzed by density gradient ultracentrifugation were processed on the afternoon of plasma collection essentially by the method of Chapman et al. (25). Sample tubes were centrifuged in an SW-41 rotor (Beckman) at 15°C for 44 h at 40,000 rpm. Completed gradients were fractionated manually using a Gilson micropipette into 400-µl fractions and stored for further analysis.

Protein mass analysis

Protein mass in gradient fractions was measured by a sodium dodecyl sulfate-modified Lowry procedure (26) using bovine serum albumin (Sigma, St. Louis, MO) as a standard.

Electrophoresis of density gradient fractions under denaturing conditions

Sodium dodecyl sulfate polyacrylamide 5–19% gradient gel elestrophoresis of density gradient ultracentrifugation fractions 1–24 was performed essentially by the method of Irwin et al. (27). The samples were loaded onto the 5–19% gradient gels together with broad range molecular weight standards (Bio-Rad, Richmond, CA) and run at 3–3.5 mA/gel (10°C) until the bromophenol blue just began to exit the gel. Gels were then stained overnight with 0.1% Coomassie Blue R-250 (Fisher Scientific) in 50% methanol, and 10% acetic acid. Gels were destained with the stain solution less Coomassie Blue

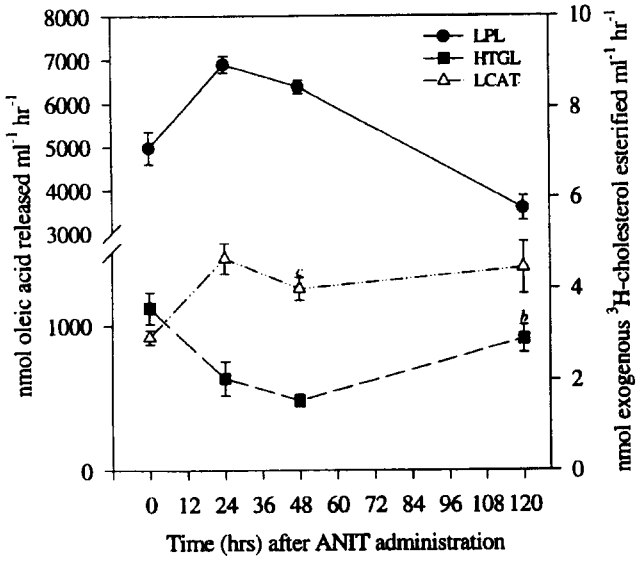

Fig. 3. Plasma lipolytic enzyme activities with respect to time after ANIT administration (100 mg/kg). Points shown are for fasted rats and are the mean ± SEM (n = 6). Lecithin:cholesterol acyltransferase (LCAT) activity was measured using an exogenous substrate (21) and lipoprotein lipase (LPL) and hepatic triacylglycerol lipase (HTGL) activities were measured using a trioleoylglycerol emulsion as substrate (22). [a]Lipoprotein lipase (LPL), [b]hepatic triacylglycerol lipase (HTGL), and [c]lecithin:cholesterol acyltransferase (LCAT) measurements were not significant ($P < 0.05$) versus controls (0 h).

and photographed. Negatives were then scanned on an AGFA Argus II using a transparency cover.

Nondenaturing gel electrophoresis of density gradient ultracentrifugation fractions

Nondenaturing 2.5–16% and 4–30% polyacrylamide gradient gels were prepared using the formulation of Asztalos et al. (28) adapted for use in an 18-cm long Bio-Rad Protein II apparatus. The loaded gels were run at 125 volts for 24 h before Coomassie blue staining. To aid in the quantification of particle sizes, high molecular weight standards (Pharmacia) of known particle diameters were run concurrently and particle diameters were estimated using a second order linear regression equation of R_f versus log (particle diameter). The gels were photographed and the negatives were scanned on an AGFA Argus II using a transparency cover.

Statistical analysis

All rat plasma data are presented as the mean of like measurements ± the standard error of the mean for the sample size. Changes in rat plasma data after ANIT treatment were assessed for statistical significance using a one-way repeated measures analysis of variance (ANOVA RM) or a Friedman repeated analysis of variance on ranks. Individual time points were further identified as significant using Dunnetts multiple comparison method ($P > 0.05$). Density gradient data was based upon single determinations of plasma from individual animals.

RESULTS

ANIT-induced reversible intrahepatic cholestasis resulted in very significant alterations in the composition of rat plasma. The major changes occurred after 18 h, peaked at 48 h and returned to near normal by 120 h. **Figure 1** shows that after 18 h the plasma total bile acid concentration increased rapidly to a peak maximum at 24 h. Bilirubin was similarly increased, reaching maximum plasma values at 48 h. In addition, ANIT-induced hepatic liver damage was characterized by significant elevations in the plasma concentration of liver enzymes. **Table 1** shows that at 48 h there was a 4-fold increase in alkaline phosphatase, 24-fold increase in aspartate aminotransferase, and 45-fold increase in alanine aminotransferase activities.

Elevations in plasma bilirubin, bile acids, and liver enzymes were followed by equally impressive increases in plasma lipids (**Fig. 2**). Elevated concentrations of plasma phospholipid and free cholesterol were observed after 18 h and were followed by maximal increases of 611% and 935%, respectively, at 48 h. The phospholipid and free cholesterol values then began to decrease to near normal values by 120 h. The elevation in plasma free cholesterol was paralleled by increases in

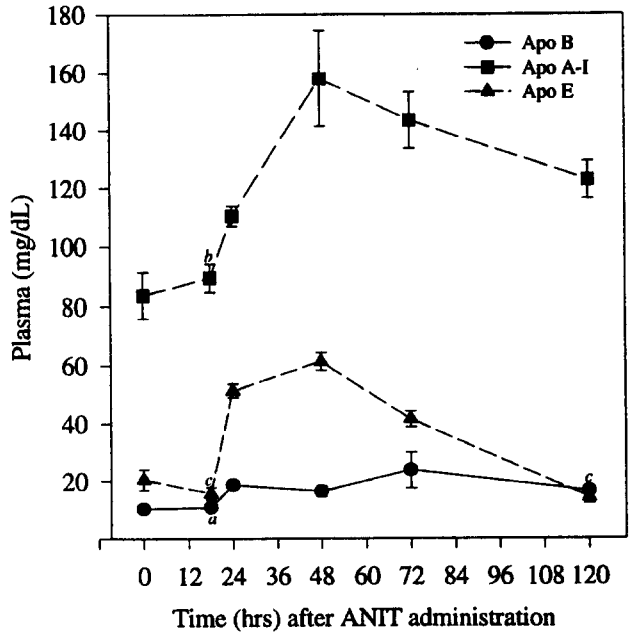

Fig. 4. Plasma apolipoprotein (apo) B, E, and A-I concentrations (mg/dL) with respect to time after ANIT administration (100 mg/kg). Points shown for fasted rats are the mean ± SEM (n = 5) and were measured by electroimmunoassay (24). [a]ApoB, [b]apoA-I, and [c]apoE measurements were not significant ($P < 0.05$) versus controls (0 h).

TABLE 2. Plasma phospholipid:apoA-I and cholesteryl ester:apoA-I ratios post-ANIT treatment

Time (h)	ApoA-I	Phospholipid	Cholesteryl Ester	Phospholipid/A-I	Cholesteryl Ester/A-I
	μM	μM	μM	*molar ratio*	*molar ratio*
0	30 ± 3	0.7 ± 0.1	0.7 ± 0.1	24 ± 5	22 ± 5
18	32 ± 2	0.9 ± .02	0.6 ± 0.1	29 ± 8	17 ± 3
24	39 ± 1	3.2 ± 0.1	1.3 ± 0.1	82 ± 6	32 ± 2
48	56 ± 5	4.3 ± 0.6	1.9 ± 0.2	77 ± 17	34 ± 6
72	51 ± 3	2.4 ± 0.2	2.2 ± 0.2	47 ± 7	44 ± 6
120	44 ± 2	0.9 ± 0.1	1.1 ± 0.1	19 ± 3	26 ± 4

Values are given as mean ± SEM (n = 5).

cholesteryl ester. However, the CE/FC ratio decreased after 18 h, to a near 1:1 mass ratio by 48 h, after which the ratio began to return towards normal. These changes occurred in the presence of normal to moderately increased LCAT activity (**Fig. 3**) such that the decrease in CE/FC ratio did not result from a deficiency in LCAT esterifying activity. Plasma triacylglycerol levels were not significantly increased as a result of cholestasis. Lipoprotein lipase activity was increased by 130% at 48 h and hepatic triacylglycerol lipase activity was decreased to 43% of control values at 48 h (Fig. 3). The phospholipase activity of hepatic lipase was not measured, but was likely affected to a similar extent.

ANIT-induced cholestasis also resulted in altered concentrations of the main rat plasma apolipoproteins B, E, and A-I. Apolipoprotein E was increased by 30-fold, apolipoprotein A-I by 19-fold, and apolipoprotein B by 1.6-fold at 48 h (**Fig. 4**) suggesting that the increased lipid mass observed in this cholestatic model was predominantly associated with apolipoprotein E and A-I and not with apolipoprotein B. The molar ratio of phospholipid to apolipoprotein A-I in plasma increased from 24 to a peak of 82 molecules phospholipid/A-I molecule by 24 h (**Table 2**). The cholesteryl ester/apolipoprotein A-I molar ratio, by contrast, rose steadily from an initial value of 22 to a peak of 44 molecules cholesteryl ester/molecule apolipoprotein A-I by 72 h (Table 2). Although not quantitated by immunoassay, sodium dodecyl sulfate polyacrylamide gel electrophoresis of density gradient fractions (see Fig. 9) indicated that apolipoprotein A-IV levels were also increased by 48 h (see Fig. 10).

Molecular species analysis by gas chromatography of the phospholipid and cholesteryl esters present during the course of ANIT-induced intrahepatic cholestasis clearly showed that the increased levels of phospholipid were due to medium chain species (**Fig. 5**), i.e., those containing a sum of 34, 36, or 38 carbons in both fatty acyl side chains, respectively. These species likely correspond, respectively, to those phospholipids containing C-16/18, C-18/18, and C-18/20 fatty acyl chains. Similar analysis of cholesteryl esters (**Fig. 6**) showed that the major cholesteryl ester species found within plasma from the ANIT-treated rat were those containing 18 and 20 carbon fatty acyl moieties. Although both C-20 and C-18 cholesteryl esters increased substantially by 48 h, the overall percentage of C-16 and C-18 esterified was increased at the expense of C-20. The percentage by mass of cholesteryl esters containing C-16, C-18, and C-20 fatty acids were 14%, 29%, and 57%, respectively, in untreated rats. In the ANIT-treated rat the respective

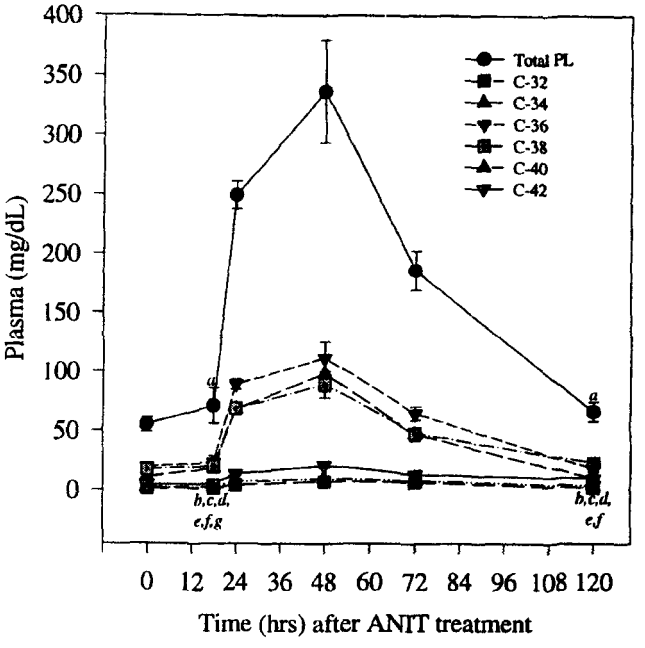

Fig. 5. Plasma phospholipid molecular species with respect to time after ANIT administration (100 mg/kg) as determined by gas chromatographic total lipid profiling (19). Points shown are for fasted rats and are the mean ± SEM (n = 6). Numbers in the legend refer to the total carbons from the two fatty acyl moieties and do not include the 3 carbons in the glycerol backbone. C-16/18, C-18/18, and C-18/20 are likely the major fatty acid combinations represented by C-34, C-36, and C-38 molecular species. [a]Total plasma phospholipid (PL), [b]C-32, [c]C-34, [d]C-36, [e]C-38, [f]C-40, and [g]C-42 phospholipid measurements were not significant ($P < 0.05$) versus controls (0 h).

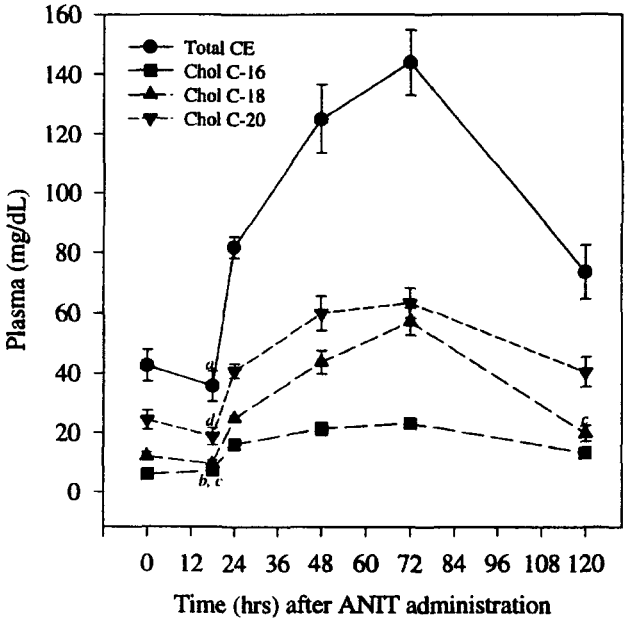

Fig. 6. Plasma cholesteryl ester molecular species with respect to time after ANIT administration (100 mg/kg) as determined by gas chromatographic total lipid profiling (19). Points shown are for fasted rats and are the mean ± SEM (n = 6). Numbers in the legend refer to total fatty acyl chain carbons and do not include carbons derived from cholesterol. [a]Total cholesteryl ester (CE), [b]C-16, [c]C-18, and [d]C-20 cholesteryl ester measurements were not significant ($P < 0.05$) versus controls (0 h).

values were 17%, 35%, and 48% at 48 h and 16%, 40%, and 44% at 72 h. The ratios returned to normal by 120 h. These results may indicate that the species-specific substrate requirements sometimes ascribed to LCAT may be more dependent upon substrate availability than a particular structural preference in this species.

As a result of the increased plasma lipids, significant alterations in the plasma lipoprotein distribution were observed. **Figure 7,** demonstrates the shift in lipoprotein mass from the HDL to the LDL density range at 48 h, the time of maximum effect. Additionally, bile acids associated with treated rat fractions were measured and are shown. Detected bile acids were most highly concentrated in the HDL density fractions and were present in fractions 8–18 and fractions above 24. It should be noted that the total lipoprotein-associated bile acid after density gradient ultracentrifugation was approximately 10% of total plasma bile acids. No bile acids were detected in control rat fractions. To further analyze the changes in lipoprotein composition, individual lipoprotein components of density gradient fractions in control and ANIT-treated rats are shown in **Fig. 8** and **Fig. 9.** Profiles of ANIT-treated rats at 24 h (Fig. 9A), 48 h (Fig. 9B), 72 h (Fig. 9C) and 120 h (Fig. 9D) revealed profound changes in the distribution of lipoproteins over the cholestatic time course when compared to the control rat profile (Fig. 8). At 24 h (Fig. 9A) there was a noticeable increase of lipid mass in the LDL density range (fractions 3–11) mainly as a result of phospholipid and free cholesterol enrichment. HDL was moderately enriched in phospholipid. At 48 h, the time point of peak plasma lipid levels, Fig. 9B, shows a marked elevation in the lipid (primarily free cholesterol and phospholipid) distributed throughout density fractions 1–24. In the LDL

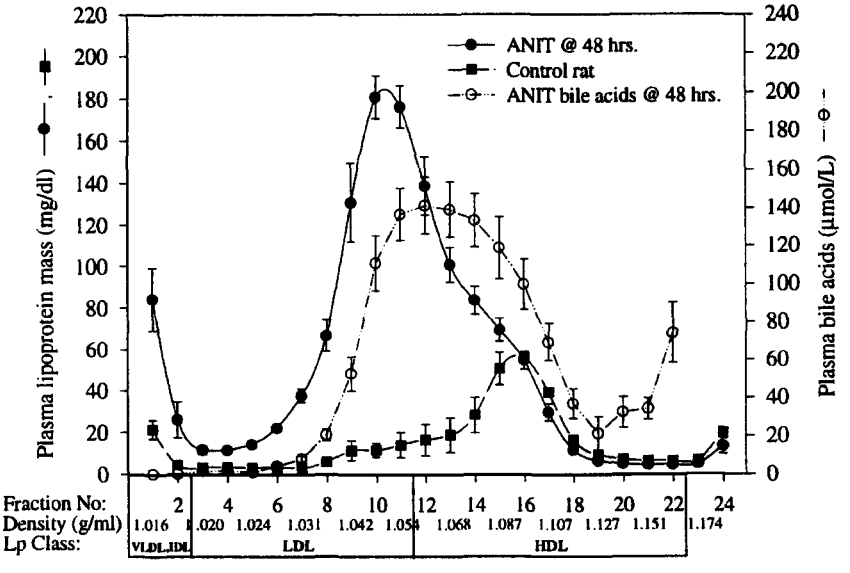

Fig. 7. Plasma lipoprotein mass (lipids plus protein) comparison after density gradient ultracentrifugation between control (n = 3) and ANIT-treated rats after 48 h (n = 4). Also shown, the distribution of bile acids (n = 4) from ANIT-treated rats after 48 h across density gradient fractions.

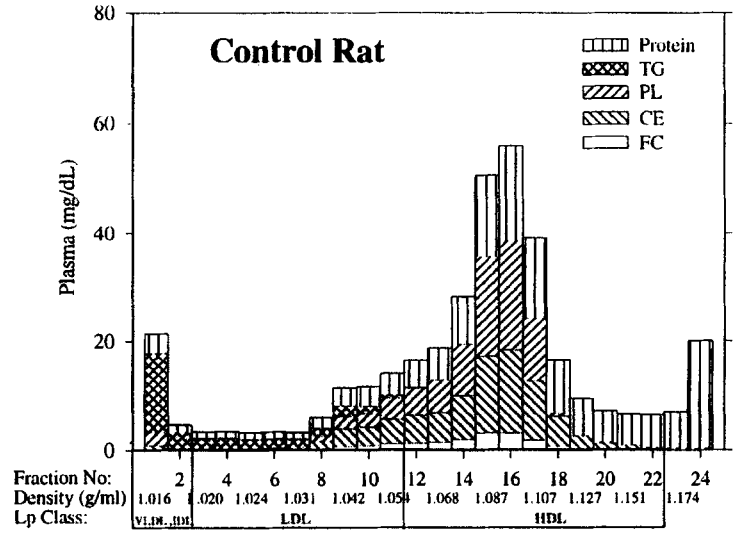

Fig. 8. Profile of untreated rat lipoprotein mass distribution after density gradient ultracentrifugation (25). Only fractions 1–24 are shown as fractions 25–30 were devoid of lipid. FC, free cholesterol; CE, cholesteryl ester; PL, phospholipid; TAG, triacylglycerol; Lp, lipoprotein.

range, (fractions 9–11), particles were particularly deficient in core neutral lipid suggesting the presence of vesicles; for example, fraction 9 is composed of FC/18%, CE/6%, PL/59%, TAG/3%, and Prot/14%. HDL (fractions 12–18) was cholesteryl ester-deficient and phospholipid-enriched when compared to control rat plasma. By 72 h (Fig. 9C), the plasma cholesteryl ester content (Fig. 2), began to return towards normal, and the lipid mass associated with the LDL region at 48 h (Fig. 9B) decreased such that there was a clearly discernible separation between the LDL and HDL density regions at fraction 13–14. The lipid composition of fractions in the LDL region (fractions 3–11) remained enriched in phospholipid. The cholesteryl ester composition of HDL was increased and there was reduced phospholipid enrichment. By 120 h (Fig. 9D) the lipid distribution returned to near normal and the excess phospholipid and free cholesterol was cleared from the plasma.

To further analyze the alterations in lipoprotein metabolism occurring at 48 h, density gradient fractions 1–24 were analyzed for apolipoprotein content by sodium dodecyl sulfate polyacrylamide gel electrophoresis on 5–19% gels. **Figure 10A,** shows the distribution throughout the gradient fractions of apolipoproteins in an untreated rat. LDL fractions 6–10 (d_{15} 1.028–1.048 g/ml), which corresponded to rat LDL, as expected contained apolipoprotein B and some apolipoprotein E. High density fractions contained increasing quantities of apolipoproteins E, A-I, and A-IV, with the major apolipoprotein E-containing fractions being fractions 11–18. Apolipoprotein A-I-rich HDL was centered around fractions 14–20 and co-fractionated with apolipoprotein A-IV. Sodium dodecyl sulfate polyacrylamide gel electrophoresis of gradient fractions 8-12 at 48 h after ANIT treatment (Fig. 10B) revealed movement of apolipoproteins A-I and A-IV into the lower density ranges. The presence of apolipoprotein B-48 in HDL fractions 13–15 suggests these rats have impaired remnant removal. The major apolipoprotein E-containing fractions were fractions 8–16, approximately 2–3 fractions less dense than that observed in an untreated rat. Apolipoprotein A-I and A-IV distribution appeared to be more wide-spread as significant amounts were found outside of the normal rat HDL density range (fractions 14–20). Additionally, fractions 8–12 that were shown by lipid analysis (Fig. 9B) to be deficient in core neutral lipid also contained a band corresponding to albumin. These results suggest an Lp-X-like vesicle may be present.

Density gradient fractions from an untreated rat and an ANIT-treated rat were subjected to nondenaturing polyacrylamide gel electrophoresis. The results are shown in **Fig. 11.** Particle diameters above 170 Å are estimates. Figure 11A shows the size distribution of lipoproteins in fractions 1–12 for an untreated rat. Fractions 1–8 were each homogeneous for a single particle size, whereas fractions 9–11 were heterogeneous and contained two populations of particles, likely LDL and a large HDL. This was not surprising given the presence of apolipoprotein B, as well as apolipoproteins E, A-I, and A-IV in these fractions (Fig. 10A). Fractions

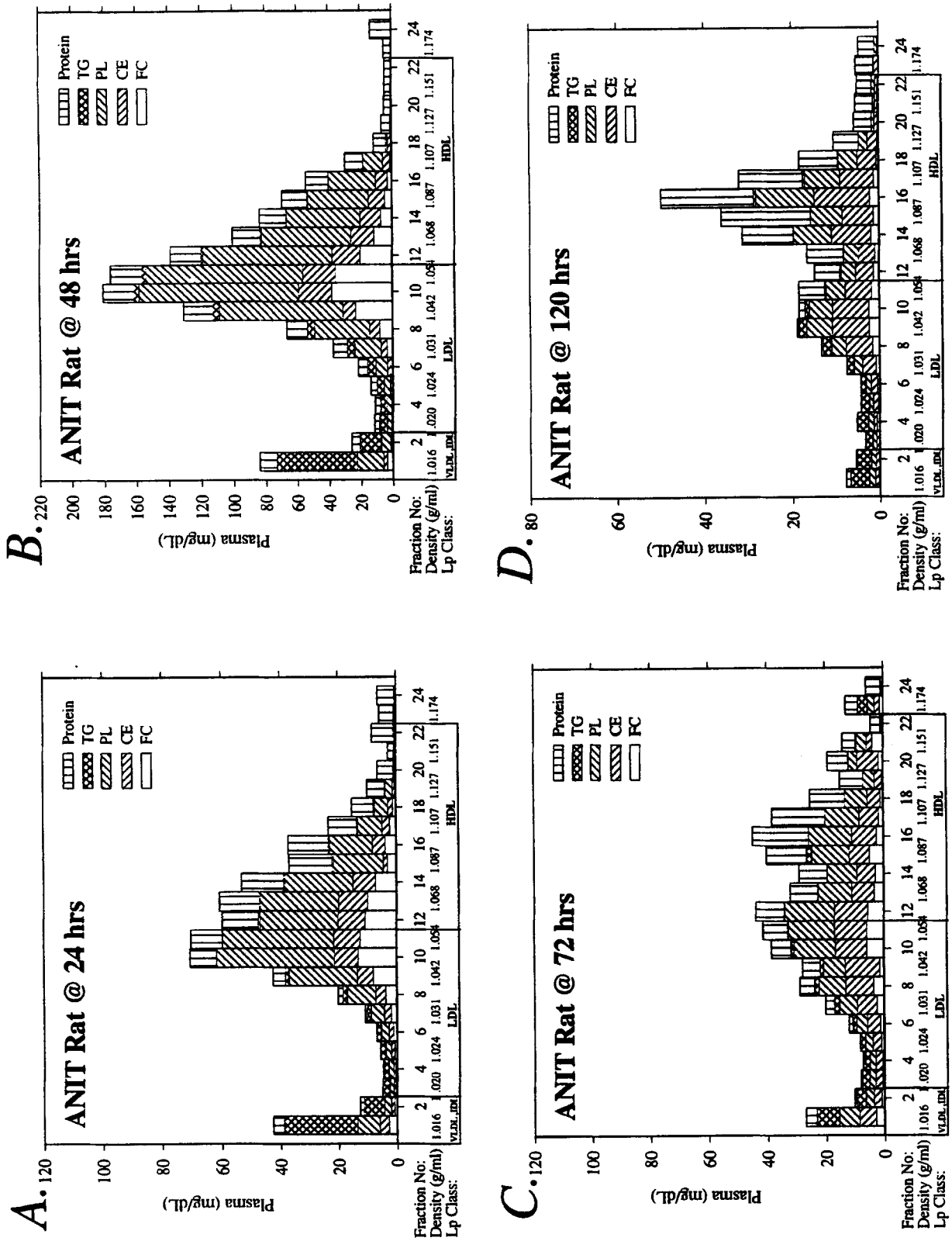

Fig. 9. Profile of rat lipoprotein mass distribution after density gradient ultracentrifugation (25). (A) 24 (B) 48, (C) 72, (D) 120 h after ANIT treatment. Only fractions 1–24 are shown as fractions 25–30 were devoid of lipid. FC, free cholesterol; CE, cholesteryl ester; PL, phospholipid; TAG, triacylglycerol; Lp, lipoprotein.

1–7 of treated rats (Fig. 11B) also contained single particle populations slightly smaller than those observed in untreated rats. This was probably due to decreased core cholesteryl esters. Fractions 9–12 of treated rats (Fig. 11B) appeared to contain at least four particle populations and these may correspond to vesicles (370–340 Å), small LDL (260 Å), VLDL and chylomicron remnants (220 Å), and a large HDL (180–140 Å). The putative LDL and HDL populations in this range appear to be smaller than their normal counterparts (Fig. 11A) probably as a result of decreased cholesteryl ester content and phospholipid enrichment. Fig. 11C and D document the particle diameters for fractions 13–24 of a control rat and an ANIT-treated rat. In general, the major differences were that the HDL from treated rats appeared to be slightly smaller in fractions 13–15 and markedly smaller in fractions 16–20. The smaller sized HDL in fractions 13–15 were likely caused by reduced cholesteryl ester content and relative phospholipid enrichment. The very small HDL in fractions 16–20 may represent discoidal particles. Additionally, as shown in Fig. 10B, apolipoprotein B-48 was present in fractions 13–16, possibly denoting impaired remnant removal and bands corresponding to these particles (Fig. 11D) may be present at the top of lanes 13–15 as the remnants may be too large to enter a 4% gel.

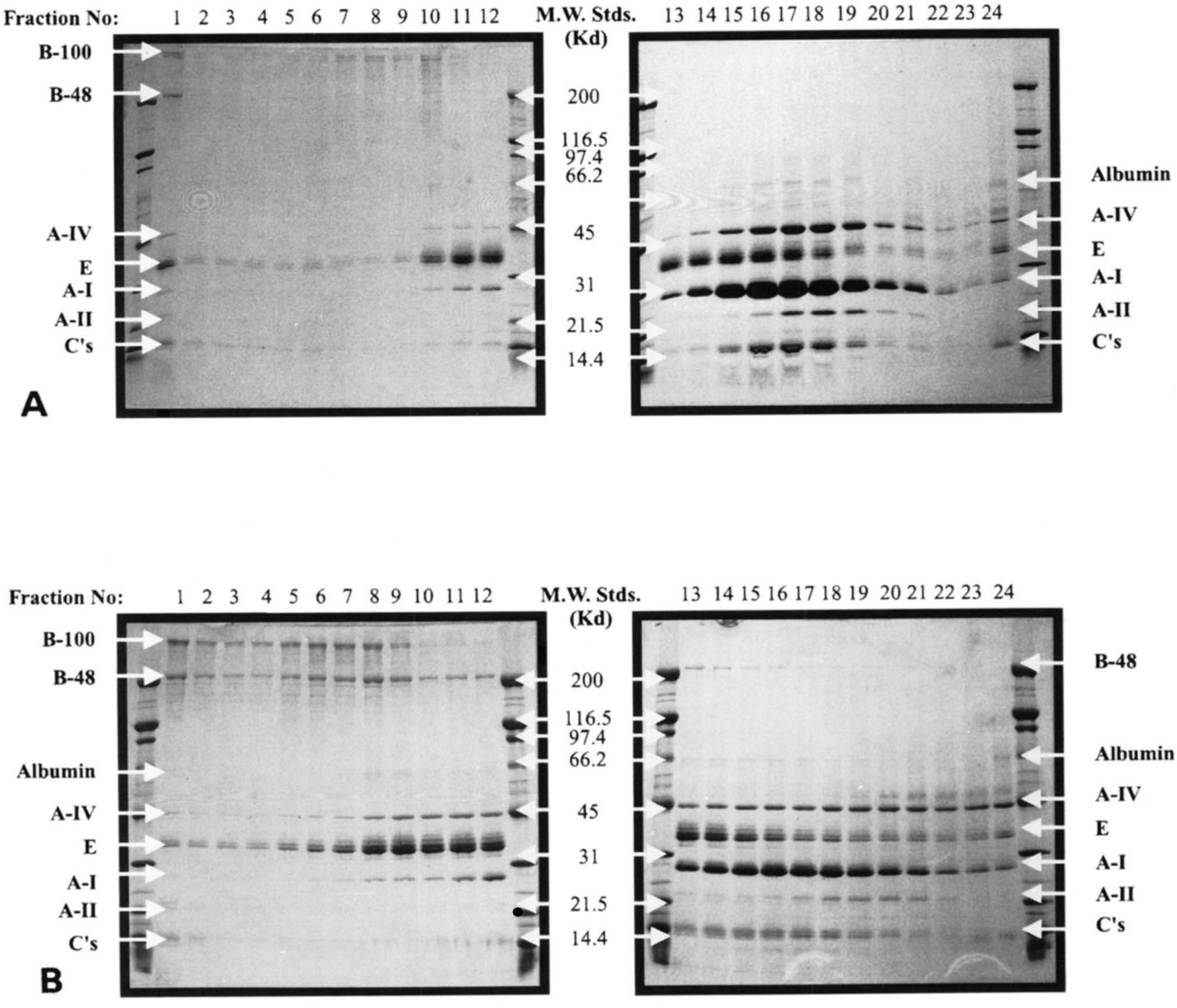

Fig. 10. Sodium dodecyl sulfate polyacrylamide gel electrophoresis of density gradient fractions after ultracentrifugation. A control rat (A) is shown as compared to an ANIT rat 48 h post-treatment (B). Twenty μg of protein was loaded in each lane (Fig. 10A, fractions 1–9 < 20 μg; Fig. 10B, fractions 1–6 < 20 μg). Molecular weight standards were broad range (Bio-Rad, Richmond, CA) of the indicated molecular weights.

DISCUSSION

Our investigation of the ANIT-treated rat as a model of intrahepatic cholestasis has clearly demonstrated marked similarities to human cholestasis, bile duct ligation, Intralipid infusion, and familial LCAT deficiency. ANIT, when administered in a single dosage (100 mg/kg by gavage in corn oil) to rats, promotes a transient, reversible intrahepatic cholestasis resulting in marked perturbations in plasma lipids and lipoproteins. The onset of cholestasis is followed by elevated levels of bile acids, bilirubin, medium chain length phospholipids, free cholesterol, and plasma enzyme markers of liver damage. All of these increased levels return to near normal by 120 h.

Although increased cholesteryl ester mass was observed, the CE/FC ratio was reduced even though LCAT activity was near normal (Fig. 3). In severe human cholestasis, hepatitis, chronic liver failure, late stage primary biliary cirrhosis (29, 30), and galactosamine-induced hepatitis in rats (31), LCAT activity is decreased. As LCAT activity is increased when hepatic damage appears to be light, such as in ANIT-treated rats, mild cases of human cholestasis and early stage primary

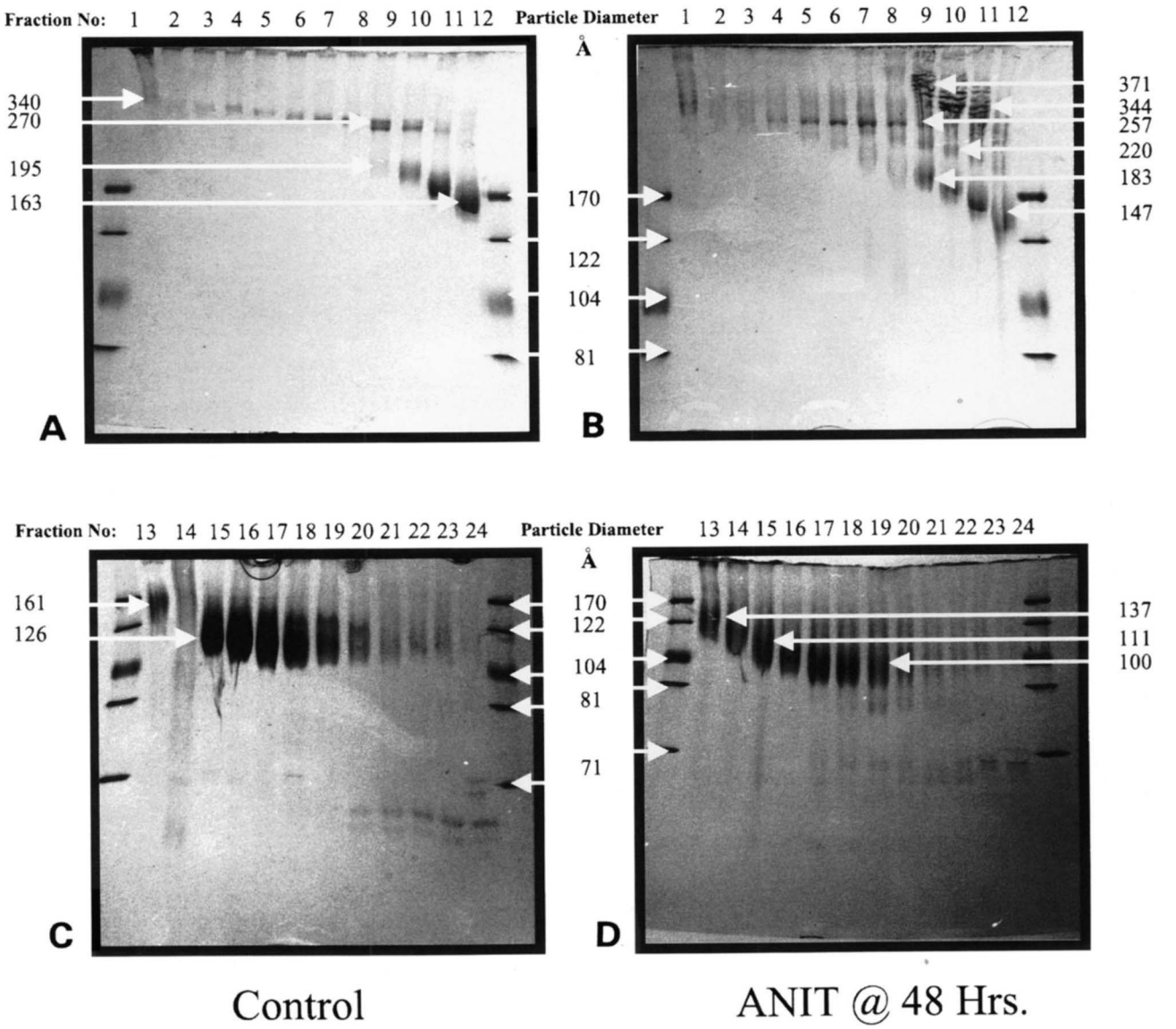

Fig. 11. Nondenaturing 2–16% polyacrylamide gradient gels of density gradient fractions 1–12 (LDL range) (Fig. 11A and B) and 4–30% polyacrylamide gradient gels of fractions 13–24 (HDL range) (Fig. 11C and D) after ultracentrifugation. A control rat (Fig. 11A and C) is shown as compared to an ANIT-treated rat 48 h post-treatment (Fig. 11B and D). Twenty μg of protein was loaded in each lane (Fig. 11A, fractions 1–9 < 20 μg; Fig. 11B, fractions 1–6 < 20 μg). Gels were stained with Coomassie Blue R-250, destained, and documented. Particle diameters above 170 Ångstroms were estimated by extrapolation using the equation of the second order regression curve of R_f verse Log (particle diameter) of high molecular weight standards (Pharmacia).

biliary cirrhosis (29, 30), the synthesis and secretion of the enzyme does not appear to be impaired. A low CE/FC ratio in the presence of near normal LCAT activity suggests that LCAT activity was either initially overloaded by the large amount of phospholipid and free cholesterol entering the plasma compartment or, alternatively, the free cholesterol and phospholipid were sequestered in particles that do not function as good LCAT substrates. The Lp-X-like particle (estimated size 340–370 Å, Fig. 11B) observed 48 h after ANIT treatment would be a likely candidate. Whether or not Lp-X is an LCAT substrate in vivo remains controversial and is probably dependent upon whether the vesicles contain significant quantities of the surface bound LCAT activating apolipoprotein, A-I. Lp-X vesicles are thought to normally contain very little if any apolipoprotein A-I (32, 33). The failure of LCAT to maintain the plasma CE/FC ratio may be due to a combination of factors which include: *1)* in the early-mid stages of ANIT treatment, much of the phospholipid and free cholesterol is localized to Lp-X-like particles and as such is not presented to LCAT in an ideal substrate form; and *2)* in order for the excess phospholipid and cholesterol to be metabolized they must either be removed by direct uptake of the Lp-X particle or be moved to appropriate HDL substrates containing the obligatory LCAT-activating apolipoproteins. Walli and Seidel (15) have demonstrated that Lp-X-containing radiolabeled core albumin can be cleared by the spleen in normal rats. Alternatively, the movement of phospholipid and cholesterol into HDL may proceed by one or both of the following mechanisms: *A)* transfer to and formation of HDL-like substrates facilitated by the binding of apolipoprotein A-I or possibly E; and *B)* phospholipid and free cholesterol movement out of Lp-X and into HDL by a gradient established as a result of LCAT-mediated depletion of HDL phospholipid and free cholesterol. Situations analogous to this have been observed in some cases of human cholestatic liver disease (29, 30), bile duct ligation (18), and Intralipid infusion (34). However, the relative importance of catabolism by tissue uptake of Lp-X as opposed to LCAT-mediated metabolism of phospholipid and free cholesterol moved into HDL remains unclear.

Lp-X vesicles may be formed by three mechanisms. *1)* In the case of some types of human obstructive liver disease, bile duct ligation, or ANIT treatment there is a reflux of biliary lipids including phospholipid and free cholesterol into the plasma compartment. Manzato et al. (32) have shown that biliary lipid complexes form Lp-X-like vesicles when albumin or plasma is added (presumably by binding bile salts) and, conversely, Lp-X can be transformed into bile-like micelles upon addition of bile salts. Studies in the perfused rat liver have shown that bile lipids are secreted in an almost constant 12:1 phospholipid:free cholesterol ratio (35); thus, for Lp-X (1:1 molar phospholipid:free cholesterol) (32) to form, extrabiliary free cholesterol must be taken up from endothelial and erythrocyte membranes as well as plasma lipoproteins and/or phospholipid must be catabolized or moved to other lipoprotein particles. Indeed Quarfordt et al. (36) have calculated that biliary lipid efflux as a result of cholestasis does not completely account for the large increases in plasma cholesterol and phospholipid usually observed. *2)* In cases of familial LCAT deficiency (37, 38), Lp-X is likely formed from the excess surface phospholipid and free cholesterol produced by lipolysis of triacylglycerol-rich chylomicrons and VLDL. The surface may simply vesicularize, trapping plasma albumin; it may then remove phospholipid and cholesterol from membranes and other lipoproteins to form the most stable particles. *3)* Infusion of 10% Intralipid into rats (34) and humans (39) results in lipolysis of the triacylglycerol-rich, phospholipid emulsion, such that a large excess of phospholipid is produced resulting in the formation of Lp-X by the same mechanism suggested for familial LCAT deficiency. In advanced cholestasis, cirrhosis, and other liver diseases, secondary LCAT deficiency would further contribute to Lp-X formation.

Ritland and Bergan (40) have shown in bile duct-ligated and cholecystectomized dogs that Lp-X is generated and that its levels vary inversely with LCAT activity. Felker et al. (17) have comprehensively evaluated the changes in lipoprotein metabolism in the plasma and perfused liver of bile duct-ligated rats. The major alterations observed were increased plasma phospholipid and free cholesterol, decreased plasma CE/FC ratio, the presence of an Lp-X-like particle, moderately increased plasma apolipoprotein B, enhanced secretion of apolipoprotein A-I, and phospholipid-enriched and cholesteryl ester-depleted HDL. As a result of the reduced CE/FC ratio and Lp-X, Felker et al. (17) speculated that LCAT activity was reduced. In contrast, others have reported increased activity (18). The similarities between the changes in lipoprotein metabolism as a result of bile duct ligation and those observed by us in the ANIT-treated rat are striking.

The role of plasma apolipoproteins in liver disease must also be considered. Plasma apolipoprotein A-I levels are increased in the ANIT-treated rat (Fig. 4), and possibly bile duct-ligated rats (17); however, they are often reduced in cases of human liver disease (41) and LCAT deficiency (37). In humans, increased catabolism of A-I has been suggested in LCAT deficiency and alcoholic hepatitis and decreased apolipoprotein A-I binding to HDL has been implicated (42). How this relates to LCAT activity and the increased apolipopro-

tein A-I levels observed in cholestatic rats remains unclear. In human LCAT deficiency and liver disease, decreased apolipoprotein A-I binding to HDL, possibly as a result of low core cholesteryl ester availability, may contribute to enhanced catabolism of this apolipoprotein. Increased apolipoprotein E levels were observed in the ANIT-treated rat and have been similarly reported in liver disease (41) and LCAT deficiency (37). Apolipoprotein E discoidal particles have been observed in LCAT deficiency and secondary LCAT deficiency resulting from liver disease (41). In the ANIT-treated rat, increased apolipoprotein E may also prove to be associated with triacylglycerol-rich lipoproteins, their remnants, and/or large HDL particles.

The appearance of apolipoprotein B-48 in the HDL density range of plasma from ANIT-treated rats (fractions 13–16, Fig. 10B) 48 h post-treatment strongly suggests the presence of either VLDL or chylomicron remnants. Defective remnant clearance in the presence of Lp-X has been noted in bile duct ligation (15, 43) and some types of human liver disease (44). Walli et al. (15), have demonstrated that Lp-X competitively inhibits remnant uptake by the hepatic apolipoprotein-E remnant receptor. However, hepatic damage may also be a factor, resulting in decreased receptor numbers and/or dysfunction.

In conclusion, the ANIT-treated rat is a transient, fully reversible, and non-surgical model of intrahepatic cholestasis. The model, like bile duct-ligated rats and dogs, many types of liver disease, Intralipid infusion, and familial LCAT deficiency, results in the genesis of abnormal lipoprotein species like Lp-X, chylomicron remnants, and phospholipid-enriched, cholesteryl ester-depleted HDL. As in bile duct ligation in rats or Intralipid infusion, and unlike many types of Lp-X positive liver disease and familial LCAT deficiency, these particles are generated in the presence of increased LCAT activity. As with any experimental rat model of lipoprotein metabolism, the differences in rat verses human lipoprotein metabolism must be considered. Certainly, this model, like the bile duct-ligated rat, is not an exact duplication of the human cholestatic situation. However, given the similarities to many aspects of human liver disease and the fact that bile duct ligation is one of the few experimental models available for the in-depth study of abnormal cholestatic lipoproteins, the ANIT-treated rat as a fully reversible, non-surgical model of abnormal lipoprotein metabolism in intrahepatic cholestasis is an important new tool.

We thank Mr. Bruce Stewart for his excellent technical assistance and analysis of rat plasma lipids by gas chromatography. This research was supported by a research grant to P. J. Dolphin from the Heart and Stroke Foundation of New Brunswick.

Manuscript received 12 December 1995 and in revised form 7 February 1996.

REFERENCES

1. Capizzo, F., and R. J. Roberts. 1971. α-Naphthylisothiocyanate (ANIT)-induced hepatotoxicity and disposition in various species. *Toxicol. Appl. Pharmacol.* **19:** 176–187.
2. Goldfarb, S., E. J. Singer, and H. Popper. 1962. Experimental cholangitis due to alpha-naphthylisothiocyanate (ANIT). *Am. J. Pathol.* **40:** 685–695.
3. Plaa, G. L., and B. G. Priestly. 1976. Intrahepatic cholestasis induced by drugs and chemicals. *Pharmacol. Rev.* **28:** 207–273.
4. Ungar, H., E. Moran, M. Eisner, and M. Eliakim. 1962. Rat intrahepatic biliary tract lesions from alpha-naphthylisothiocyanate. *Arch. Pathol.* **73:** 427–435.
5. Desmet, V. J., B. Krstulovic, and B. Van Damme. 1968. Histochemical study of rat liver in α-naphthylisothiocyanate (ANIT)-induced cholestasis. *Am. J. Pathol.* **52:** 401–421.
6. Kosser, D. C., P. C. Meunier, J. A. Handler, R. S. Sozio, and R. S. Goldstein. 1993. Temporal relationship of changes in hepatobiliary function and morphology in rats following α-naphthylisothiocyanate (ANIT) administration. *Toxicol. Appl. Pharmacol.* **119:** 108–114.
7. El-Hawari, A. M., and G. A. Plaa. 1979. Impairment of hepatic mixed-function oxidase activity by α- and β-naphthylisothiocyanate: relationship to hepatotoxicity. *Toxicol. Appl. Pharmacol.* **48:** 445–458.
8. Schaffner, F., H. H. Scharnbeck, F. Hutterer, H. Denk, H. A. Greim, and H. Popper. 1973. Mechanism of cholestasis. VII. α-Naphthylisothiocyanate-induced jaundice. *Lab. Invest.* **28:** 321–331.
9. Plaa, G. L., L. A. Rogers, and J. R. Fouts. 1965. Effect of acute alpha-naphthylisothiocyanate administration on hepatic microsomal drug metabolism in the mouse. *Proc. Soc. Exp. Biol. Med.* **119:** 1045–1048.
10. Becker, B. A., and G. A. Plaa. 1965. Quantitative and temporal delineation of various parameters of liver dysfunction due to α-naphthylisothiocyanate. *Toxicol. Appl. Pharmacol.* **7:** 708–718.
11. Becker, B. A., and G. L. Plaa. 1965. The nature of α-naphthylisothiocyanate-induced cholestasis. *Toxicol. Appl. Pharmacol.* **7:** 680–685.
12. Krell, H., H. Hoke, and E. Pfaff. 1982. Development of intrahepatic cholestasis by α-naphthylisothiocyanate in rats. *Gastroenterology.* **82:** 507–514.
13. Katterman, V. R., and D. I. Wolfrum. 1970. Cholesterinstoffwechsel und Lecithin-Cholesterin-Acyltransferase im Plasma bei experimenteller Hepatitis and Cholestase and der Ratte. *Z. Clin. Chem. Klin. Biochem.* **8:** 413–419.
14. Cooper, A. D., and R. K. Ockner. 1974. Studies of hepatic cholesterol synthesis in experimental acute biliary obstruction. *Gastroenterology.* **66:** 586–595.
15. Walli, A. K., and D. Seidel. 1984. Role of lipoprotein-X in the pathogenesis of cholestatic hypercholesterolemia: uptake of lipoprotein-X and its effect on 3-hydroxy-3-methylglutaryl coenzyme A reductase and chylomicron remnant removal in human fibroblasts, lymphocytes, and in the rat. *J. Clin. Invest.* **74:** 867–879.
16. Mitamura, T. 1984. Alterations of high density lipoproteins in experimental intrahepatic cholestasis in the rat

induced by administration of α-naphthylisothiocyanate. *J. Biochem.* **95:** 29–36.

17. Felker, T. E., R. L. Hamilton, J. Vigne, and R. J. Havel. 1982. Properties of lipoproteins in blood plasma and liver perfusates of rats with cholestasis. *Gastroenterology.* **83:** 652–663.
18. Calandra, S., M. J. Martin, M. J. O'Shea, and N. McIntyre. 1972. The effect of experimental biliary obstruction on the structure and lipid content of rat erythrocytes. *Biochim. Biophys. Acta.* **260:** 424–432.
19. Kuksis, A., J. J. Myher, K. Geher, A. G. D. Hoffman, W. C. Breckenridge, G. J. L. Jones, and J. A. Little. 1978. Comparative determination of plasma cholesterol and triacylglycerol by automated gas–liquid chromatographic and Autoanalyzer methods. *J. Chromatogr.* **146:** 393–412.
20. Chen, C-H., and J. J. Albers. 1982. Characterization of proteoliposomes containing apoprotein A-I: a new substrate for the measurement of lecithin:cholesterol acyltransferase activity. *J. Lipid Res.* **23:** 680–691.
21. Jauhiainen, M., and P. J. Dolphin. 1986. Human plasma lecithin-cholesterol acyltransferase: an elucidation of the catalytic mechanism. *J. Biol. Chem.* **261:** 7032–7043.
22. Jackson, R. I., and L. R. MacLean. 1991. Human postheparin plasma lipoprotein lipase and hepatic triglyceride lipase. *Methods Enzymol.* **197:** 339–345.
23. Nilsson-Ehle, P., and M. C. Schotz. 1976. A stable, radioactive substrate emulsion for the assay of lipoprotein lipase. *J. Lipid Res.* **17:** 536–541.
24. Krul, E. S., and P. J. Dolphin. 1982. Isolated hepatocytes from hypercholesterolemic rats secrete discoidal lipoproteins. *FEBS Lett.* **139:** 259–264.
25. Chapman, M. J., S. Goldstein, S. Lagrange, and P. M. Laplaud. 1981. A density gradient ultracentrifugal procedure for the isolation of the major lipoprotein classes from human serum. *J. Lipid Res.* **22:** 339–356.
26. Markwell, M. A., S. M. Haas, L. L. Bieber, and N. E. Tolbert. 1978. A modification of the Lowry procedure to simplify protein determination in membrane and lipoprotein samples. *Anal. Biochem.* **87:** 206–210.
27. Irwin, D., P. A. O'Looney, E. Quinet, and G. V. Vahouny. 1984. Application of SDS gradient polyacrylamide slab gel electrophoresis to analysis of apolipoprotein mass and radioactivity of rat lipoproteins. *Atherosclerosis.* **53:** 163–172.
28. Asztalos, B. F., C. H. Sloop, L. Wong, and P. S. Roheim. 1993. Two-dimensional electrophoresis of plasma lipoproteins: recognition of new apoA-I-containing subpopulations. *Biochim. Biophys. Acta.* **1169:** 291–300.
29. Ritland, S., J. P. Blomhoff, and E. Gjone. 1973. Lecithin:cholesterol acyl-transferase and lipoprotein-X in liver disease. *Clin. Chim. Acta.* **49:** 251–259.
30. Wengeler, H., H. Greten, and D. Seidel. 1970. Serum cholesterol esterification in liver disease. Combined determinations of lecithin:cholesterol acyltransferase and Lp-X. *Eur. J. Clin. Invest.* **2:** 372–378.
31. Sabesin, S. M., L. B. Kuiken, and J. B. Ragland. 1975. Lipoprotein and lecithin:cholesterol acyltransferase changes in galactosamine-induced rat liver injury. *Science.* **190:** 1302–1304.
32. Manzato, E., R. Fellin, G. Baggio, S. Walch, W. Neubeck, and D. Seidel. 1976. Formation of lipoprotein-X: its relationship to bile compounds. *J. Clin. Invest.* **57:** 1248–1260.
33. Patsch, J. R., K. C. Aune, A. M. Gotto, and J. D. Morrisett. 1977. Isolation, chemical characterization and biophysical properties of three different abnormal lipoproteins: Lp-X_1, Lp-X_2, and Lp-X_3. *J. Biol. Chem.* **252:** 2113–2120.
34. Breckenridge, W. C., G. Kakis, and A. Kuksis. 1979. Identification of lipoprotein X-like particles in rat plasma following Intralipid infusion. *Can. J. Biochem.* **57:** 72–82.
35. Baumgartner, U., J. Scholmerich, P. Leible, and E. H. Farthmann. 1992. Cholestasis, metabolism and biliary lipid secretion during perfusion of rat liver with different bile salts. *Biochim. Biophys. Acta.* **1125:** 142–149.
36. Quarfordt, S. H., H. Oelschlaeger, W. R. Krigbaum, L. Jakoi, and R. Davis. 1973. Effect of biliary obstruction on canine plasma and biliary lipids. *Lipids.* **8:** 522–530.
37. Guerin, M., P. J. Dolphin, and M. J. Chapman. 1993. Familial lecithin:cholesterol acyltransferase deficiency: further resolution of lipoprotein particle heterogeneity in the low density interval. *Atherosclerosis.* **104:** 195–212.
38. Torsvik, H., K. Berg, H. N. Magnani, J. McConathy, P. Alaupovic, and E. Gjone. 1972. Identification of the abnormal cholestatic lipoprotein (Lp-X) in familial lecithin:cholesterol acyltransferase deficiency. *FEBS Lett.* **24:** 165–168.
39. Tashiro, T., Y. Mashima, H. Yamamori, K. Horibe, M. Nishizawa, M. Sanada, and K. Okui. 1991. Increased lipoprotein-X causes hyperlipidemia during intravenous administration of 10% fat emulsion in man. *J. Parenter. Enteral Nutr.* **15:** 546–550.
40. Ritland, S., and A. Bergen. 1975. Plasma concentration of lipoprotein-X in experimental bile obstruction. *Scand. J. Gastroenterol.* **10:** 17–24.
41. Clifton, P. M., P. J. Barter, and A. M. Mackinnon. 1988. High density lipoprotein particle size distribution in subjects with obstructive jaundice. *J. Lipid Res.* **29:** 121–135.
42. Seidel, D., H. Greten, H. P. Geisen, H. Wengeler, and H. Wieland. 1972. Further aspects on the characterization of high and very low density lipoproteins in patients with liver disease. *Eur. J. Clin. Invest.* **2:** 359–364.
43. Larsson, B., and A. Nilsson. 1980. Inhibition of chylomicron remnant uptake in cholestatic rat. *Scand. J. Gastroenterol.* **15:** 959–967.
44. Muller, P., R. Fellin, J. Lamprecht, B. Agostini, H. Wieland, W. Rost, and D. Seidel. 1974. Hypertriglyceridemia secondary to liver disease. *Eur. J. Clin. Invest.* **4:** 419–428.